Composite Structures 251 (2020) 112625

Contents lists available at ScienceDirect

Composite Structures

journal homepage: www.elsevier.com/locate/compstruct

Cryogenic drilling of carbon fibre reinforced thermoplastic and thermoset polymers

Marcelo Ferreira Batista *, Igor Basso, Francisco de Assis Toti, Alessandro Roger Rodrigues, José Ricardo Tarpani

São Carlos School of Engineering, University of São Paulo, Brazil

A R T I C L E I N F O

Keywords:
CFRP
Cryogen
Drilling
Delamination
Damages

A B S T R A C T

Carbon fibre reinforced polymers (CFRP) are suitable materials for high-end applications due to the high strength to weight ratio. This important advantage counteracts to their machinability because the inherent anisotropy and the heterogeneity lead a high difficulty to reach good quality in terms of surface integrity, dimensional and geometrical tolerances. Hereupon, this paper determines the effect of the cryogenic and dry drilling as well as tool feed rate on delamination, uncut fibres, hole diameter and roundness when applying thermoplastic and thermoset CFRP as workpiece material. Scanning electron microscopy (SEM), and specific cutting and thrust energies aided to explain the damages' phenomena. The results showed that hole quality varies along hole depth and depends both on composite's matrix and drilling strategy. Delamination and uncut fibres are distinct at the hole entrance and exit since they depend on surrounding matrix/fibre layers. Cryogenic drilling reduced both delamination at the hole exit and uncut fibres at the hole entry for the thermoset materials. Finally, the variation in hole diameter and roundness was minimized when drilling thermoplastic matrix by using cryogenic cooling.

1. Introduction

Carbon Fibre Reinforced Polymers (CFRP) are widely used in aeronautics and high-end applications. Possible reductions in production costs can lead to an increase in the application of CFRP in industries for mass production, such as automotive [1–3]. However, despite the components in CFRP are usually manufactured near net shape [3], at the end of production chain some cutting operations are unavoidable. Drilling is the most common operation for assembly of components by riveting and bolting. Holes with low level of damages are still a challenge in CFRP given its characteristics e.g. high structural stiffness, abrasive nature of fibres, anisotropic behaviour and laminate constitution. Cracks, fibre pull out, burrs, and delamination are recurrent damages after drilling operation and can affect either the structure or assembly of components [4–6].

Besides the low thermal conductivity of polymers, the temperature in the cutting zone during the machining of CFRP can easily exceed both glass transition and degradation temperatures due to the heat generated around the tool edge . This increase of the temperature accelerates the tool wear and affects the stiffness of both composites with thermoset and thermoplastic matrices [5–8]. During the drilling the reached maximum temperature and heat dissipation depend on the resin and reinforcement types as well as on the cutting speed and tool feed [9–12]. This can lead to a matrix stability reduction, stress concentration and thermal damages such as matrix smearing and material loss [9,10]. As a consequence, hole quality is impaired since damages like chipping, porosity and uncut fibres can take place [4,11]. The temperature reaches the maximum peak in the hole wall near the drill exit which in turn facilitates the push out delamination mainly when using worn tools [11,12]. Delamination, uncut fibres, cracks and porosities increased as temperature also elevated after drilling T300 carbon fibre with AG80 epoxy matrix. Furthermore, the increase of temperature directly affects the number of damaged layers [4].

The use of cryogenic cooling in metals drilling is well known as good strategy to improve the roughness and reduce the tool wear [13], as well as to mitigate the burr formation due to ductility decreasing. Moreover, the cooling can avoid the built up edge (BUE) which in turn can lead to an inferior quality surface, higher dimensional deviations and greater probability of drill catastrophic failure [13]. When compared to conventional cooling, cryogenic machining is an environmental-friendly method, trends to improve the production rate by increasing cutting speed and tool feed, upgrades surface quality and

* Corresponding author.
E-mail address: mfb@usp.br (M. Ferreira Batista).

https://doi.org/10.1016/j.compstruct.2020.112625
Received 18 November 2019; Revised 4 April 2020; Accepted 9 June 2020
Available online 18 June 2020

increases tool life. All these benefits justify the initial costs of the cryogenic machining [14].

Cooling strategies in machining of composites were evaluated in some studies [13,15–17] aiming to reduce the temperature and consequently damages in fibre reinforced polymer (FRP). The cryogenic cooling in polymers allows withstanding the cutting forces and reducing the deformation by means of tribological conditions improvements [14]. A comparative study between Minimum Quantity Lubrication (MQL) and Liquid Nitrogen (LN_2) as cooling strategies shows that a reduction of the cutting temperature minimizes burr formation and hole roundness when drilling Glass Reinforced Fibre Aluminium Laminate (GLARE), however the behaviours were distinct at the hole entry and exit [15]. Dimensional variation was reported by justifying that the use of cryogenics increases fibre stiffness and reduces its flexion, i.e., less contraction after thermal expansion [15]. An improvement in the circularity was also reported in cryogenic condition when compared to dry drilling and MQL. For both dry and MQL drilling, the nominal values of the hole diameter were smaller than the nominal drill diameter because of the matrix thermal retraction regardless of cutting speed (v_c) and feed rate (v_f) used [15].

Higher drill feeds increase both thrust force and hole exit delamination [18–20]. When applying cryogenic cooling this effect on thrust force (feed force) and torque during CFRP drilling is amplified [17]. It suggests that mechanical properties increase under low temperature, such as modulus of elasticity and the maximum tensile stress. As a consequence of this increase in thrust force and torque, delamination factor (F_d) also grew up. On the other hand, the hole walls presented superior quality containing less pull out, cracks, matrix fusion; also hole diameters tended to the nominal one and presented less variability. In addition, cryogenic cooling reduced substantially both cutting edge honing and tool wear. Due to this wear decreasing, delamination was more constant when using cryogenic cooling [17].

Therefore, cryogenic cooling applied to drill CFRP has showed some advantages when compared to dry condition (room temperature ~25 °C) manly regarding the tool life [17]. When focusing hole's quality, such as reduction of delamination and burr, cryogenic machining still needs a better understanding of the damage mechanisms. In addition, comparisons among different cooling techniques to drill thermoplastic and thermoset CFRP were not found in scientific literature. Thus, this paper determines the effect of the cryogenic and dry drilling on hole surface integrity of thermoset and thermoplastic CFRP. Damages were characterized by SEM images and their mechanisms are explained. Drill feed was also varied to evaluate its interaction with cooling method over hole damages. All quantitative results were analysed statistically by Analysis of Variance given their intrinsic variability when machining composites.

2. Experimental procedures

2.1. Materials and cutting conditions

Two different composite laminate systems with nominal fibre to resin ratio by volume of 50:50 were evaluated in this study. The first one was a 5 mm-thick laminate comprising continuous carbon fibre reinforced thermoplastic poly-phenylene sulphide (PPS-C) fabricated at industrial scale via hot compressing (300 °C) 16 layers of 0/90° bidirectional 5 harness satin (5HS) fabric semi-impregnated with PPS (Tencate™) stacked to $[(0/90)/\pm 452/(0/90)]_4$ array. The second material was a 5 mm-thick laminate comprising continuous carbon fibre reinforced epoxy resin (EPX-C) also manufactured at industrial-scale via vacuum bag autoclave processing 24 layers of 0/90° bidirectional plain-weave fibre fabric (Hexcel™) pre-impregnated with EPX system (Araldite LY 5052 resin and Aradur 5052 polyamines mixture also supplied by Hexcel™) piled up to $[(0/90)/\pm 452/(0/90)]_6$ architecture and subsequently cured at 180 °C. The Table 1 exhibits the

Table 1
Fibre fabrics characteristics.

Material	grammage [g/m^2]	beams by inch	filaments by beams
PPS-C	280	17.8 × 17.8	3,000
EPX-C	193	11.5 × 11.5	3,000

fibre fabrics characteristics and the Table 2 exhibits the matrices' thermal properties.

The drilling process was carried out with 60 m/min cutting speed. Four feeds per rotation and two conditions of cooling, totalizing 8 different conditions for each workpiece material. Each condition was tested 3 times. Exploratory tests were carried out before final experimental matrix definition in order to classify the significant inputs. By employing Analysis of Variance with 5% significance level the results indicated that cutting speed and drill wear did not influence on hole damages which in turn can also be validated by [9,18,21]. Particularly, no tool wear took place after drilling 48 holes. Table 3 shows all experimental parameters and responses aimed.

2.2. Experimental apparatus and setup

Three-axis Romi D800 machine centre with 10,000 maximum rotation, 20 m/min maximum feed rate and 20 CV power was used for drilling tests. A 6 mm diameter solid carbide twist drill coated with diamond was used (code A1163-6, Seco Tools S/A). This drill has two point angles being the first with 130° and the second with 60°. In all tests the thrust force and torque were acquired by a 9272 4-component Kistler dynamometer. The operating temperature range of the dynamometer is from 0 °C to 70 °C, so it does not tolerate cryogenic temperature. Therefore, the drill was fixed over the dynamometer in a special fixture and the liquid nitrogen (LN_2) nozzle was positioned above the drill point and upward directed to the specimen. The specimen was fixed in the machine spindle. A K-type thermocouple connected to the Fluke multimetr model 69 IV was used to verify the drill temperature at 10 mm below its tip after each drilled hole. The Fig. 1 presents the drilling set up. The cryogenic system model SC-18 (Semper Crio S/A) was used to apply the LN_2 during the drilling operations at 100 kPa exhaustion pressure.

A 4-channel amplifier Kistler model 5019 was used to amplify the dynamometer signals. A 5 kHz sampling rate was used to avoid the aliasing phenomenon and to attend to the Nyquist frequency, Eq. (1).

$$SR > 2f_{exc} > 2(1000 \cdot z \cdot v_c/60 \cdot \pi \cdot D) \tag{1}$$

in which SR is the sampling rate (H_z), f_{exc} is the excitation frequency (H_z), z is the number of drill teeth, v_c is the cutting speed (m/min) and D is the drill diameter (mm). Force and torque signals were digitalized, conditioned and processed using a National Instruments board model BNC 2110, a Labview 7.1™ and Matlab 2014a™ (V 8.3.0.532) routines, respectively.

The hole external surfaces and damages were observed by employing the Axiotech Carl Zeiss and the 3D Olympus OLS4100 microscopes. This latter was also used to measure the edge radii and to validate the exploratory drilling tests in which no drill wear occurred. The pictures were loaded into a CAD® (2007) software, then the external damages (delamination and uncut fibres) were quantified. Hole diameter and roundness were measured by Starret model MVR300 visual system and MetLogix® software. The hole microscopic images were obtained in the Inspect F50 Scanning Electron Microscope (SEM).

Fig. 2 presents the edge radii images and their measurements. The rake angle (γ) is more positive and the edge radius is sharper at the 60° tool tip angle (Fig. 2c). On the contrary, the rake angle at the 130° tip angle is smaller and the edge radius is almost twice greater than those at the 60° tool tip angle (Fig. 2b). Finally, the edge radius at the drill centre (chisel edge) is the same order of magnitude from 130° tool tip

Table 2
Matrix thermal properties.

Material	thermal conductivity [W/m.K]	thermal expansion [µm/m.k]	specific heat [J/kg.K]	glass transition [C°]
PPS	0,25	1000	50–70	85–95
EPX	0,2	1500	100	120

Table 3
Experimental matrix.

Control factor (input)	Levels	Response (output)
Feed [mm/rev]	0.045; 0.090; 0.180; 0.360	Delamination factor (F_d) [*] Uncut fibres (UCF) [*]
Work Material	EPX-C and PPS-C	Thrust force [N] Torque [N.cm]
Cooling method	dry (room temperature) and cryogenic (LN_2-liquid nitrogenous)	Hole diameter [mm] Hole roundness [µm] SEM images
Replications	3	

* Dimensionless.

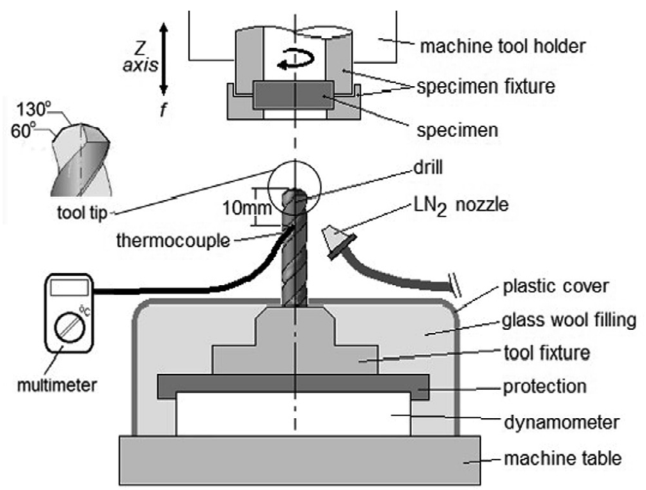

Fig. 1. Schematic drilling setup.

angle (Fig. 2a). In this case, chip formation is switched by compressive strain of the workpiece material especially at low cutting speed given the tiny chisel diameter (~∅0.095 mm).

2.3. Statistical analysis and hole quality criteria

Analysis of Variance (ANOVA) was applied to determine the effects of the control factors (cooling method, tool feed and workpiece material) on responses (delamination, uncut fibres, hole diameter and roundness). The Statistica™ (12) software was used to proceed a factorial analysis with multiple variables for main factors and 2nd order interactions by adopting a 5% significance level. The normality and residuals of all data were properly checked. Thus, the results are independent and evenly distributed (no systematic error). In Results section, significant p-Values ($p < 0.05$) will be bolded in tables while vertical bars will represent 95% confidence interval in graphs of the main effects and interactions.

Delamination factor (F_d) [22] was used to evaluate the delamination at the entry and exit of the holes. F_d is the ratio between the maximum diameter (D_{max}) at the major delamination zone and the nominal diameter (D_{nom}), Eq. (2), as shown in Fig. 3a.

$$F_d = D_{max}/D_{nom} \tag{2}$$

Other damage with expressive occurrence is the uncut fibre, designated as UCF in this paper. Uncut fibre is a portion of fibre that was not sheared and remains after the drilling process (Fig. 3b). This type of damage was already presented as fuzzing [23] and recently named as burr [20]. It is an undesirable damage because negatively affects either bolt or rivet fitting during assembly of composite components. UCF value is defined in this paper as the ratio between the sum of *n* arc segments (yellow lines in Fig. 3b containing uncut fibres and the total arc or hole perimeter, Eq. (3).

$$UCF = \sum_{i=1}^{n} arc_i/\pi \cdot D_{nom} \tag{3}$$

As above-mentioned, besides delamination factor and uncut fibres, hole diameter and roundness were also evaluated. These criteria are non-destructive methods generally used industrially [3]. After these analyses, the holes were axially cut to investigate the morphological features of their walls by examining SEM images.

X ray computed tomography (CT) and Ultrasound (UT) have been used as technique to quantify the internal damages in the CFRP holes [19,24,25]. Although they are non-destructive methods, Scanning Electron Microscopy (SEM) was used in this paper aiming to identify

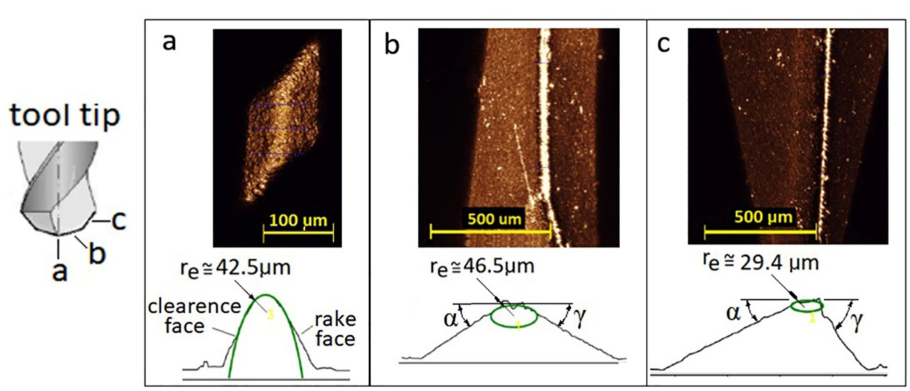

Fig. 2. Tool tip edge radius in (a) chisel edge, (b) 130° tool tip angle, and (c) 60° tool tip angle.

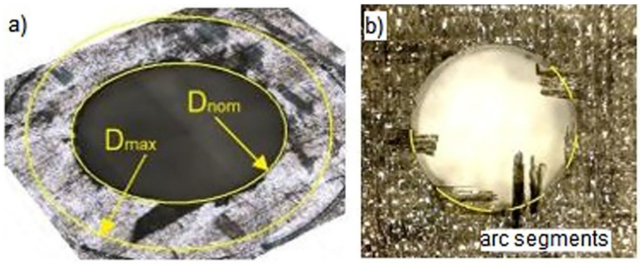

Fig. 3. Damages and measures: (a) D_{max} and D_{nom} and (b) arc segments of uncut fibres.

visually the damages mechanisms at the hole entrance and exit borders.

3. Results and discussion

3.1. Forces, torque and specific energies

Fig. 4 presents how the drilling process occurs and compares the thrust force (Ft) and torque (Mt) measured at each step for both composite materials and cooling methods. This is helpful to understand the drilling phenomenon.

At the step I, the first tool tip angle (130°) entries into the specimen and the chisel edge imposes a high thrust force that increases sharply, also verified by Jia et al. [26]. In the step II, the second tool tip angle (60°) engages, the thrust force keeps raising but slightly. At the third step, the entire drill tip is engaged and the thrust force reaches a maximum value due to the maximization of the shear plane. During the steps II and III the thrust force presents small oscillations because the drill crosses the matrix and fibres layers [24]. At the step IV, the drill point starts to exit and the thrust force drops sharply; then the second point angle starts to exit and thrust force keeps decreasing at low rate in the step V. At the step VI, the thrust force is minimally negative meaning that the workpiece material induces a compressive force against the drill secondary edges, i.e., tool return non-free (with friction).

Drill edges were fully engaged at the end of step II, where the torque should reach the maximum value. However, the torque raises slightly and reaches the maximum value after the end of hole (5 mm deep) where the tool is totally engaged into the workpiece material [12,27]. Then the torque decreases slightly although the major edges are no longer in contact with specimen. Besides torque generated by cutting phenomenon, the drill external diameter engages and rubs the hole wall as already verified using acoustic emission [28]. An increase of temperature is due to the torque, i.e., according to Sorrentino et al. [12] the heating of the process leads to a thermal expansion of the workpiece. After step V the torque does not decrease immediately confirming that the drill keeps rubbing inside hole. The temperature decreases very slowly given the low dissipation of the thermal energy in the matrix, even with the better thermal conductivity of the fibres [12,29]. In addition, these differences of thermal conductivity between matrix and fibre can lead to a compressive stress in the fibres [30], increasing the damages and their propagation.

Fig. 5a and Fig. 5b present the difference of thrust force (F_t) for dry and cryogenic cooling when drilling EPX-C and PPS-C, respectively, for 0.045 and 0.360 mm/rev feed. In the cryogenic cooling at 0.360 mm/rev feed, the maximum thrust force was 27% and 22% greater than in dry condition for EPX-C and PPS-C laminates, respectively. At 0.045 mm/rev feed, the cryogenic cooling increased 50% and 45% the maximum thrust force when drilling EPX-C and PPS-C materials, respectively. Therefore, the lowest drill feed allows longer exposure time and consequently higher reduction of temperature in the material. Both cases prove that the cryogenic cooling raises the mechanical strength of the workpiece. In the first step of drilling (first tool tip contact) in Fig. 5a and Fig. 5b, the slope of thrust force is greater for cryogenic than for dry condition, so the stiffness is increased by cryogenic cooling.

As aforementioned and showed in Fig. 4, the main drill lips are already engaged at step II. However, the torque keeps raising after that, indicating that an additional torque can be from friction between drill secondary edge and hole wall; this torque keeps increasing even with drill penetration since contact area also enhances. As known for metals, this promotes an increase in the temperature. In polymers this temperature growth is extremely harmful because it can promote a thermal expansion of the material which affects the holes diameter and roundness, as will be demonstrated in Section 3.2 ahead. A reduction in the temperature improves the mechanical strength and stiffness of the composite, as previously mentioned. Moreover, the cryogenic cooling reduces the thermal expansion so that friction of the secondary edges causes additional torque.

For cooling methods, similar trends were observed in the torque (Fig. 6); under cryogenic method, the torque is higher than that for dry method due to the increase of the stiffness for both composites,

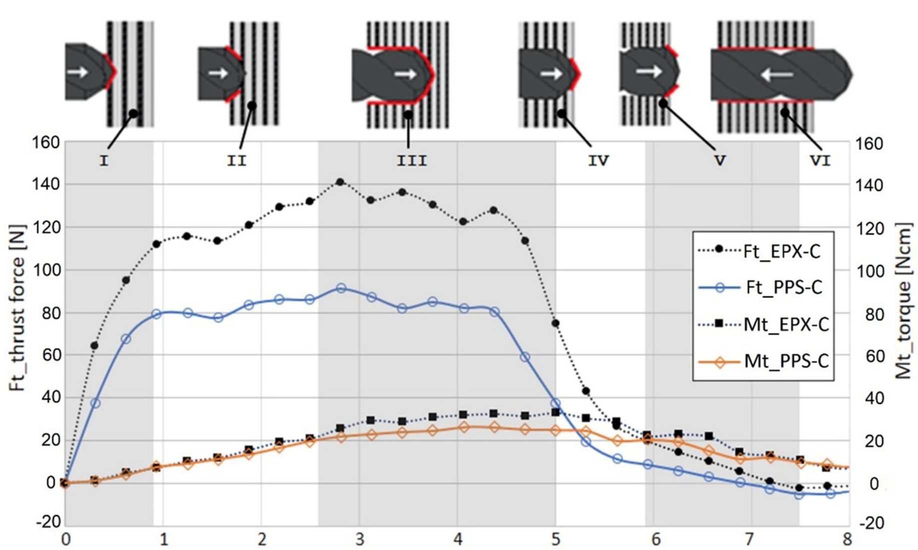

Fig. 4. Thrust force and torque comparison at each step (I to VI) of drilling for PPS-C and EPX-C (0.360 mm/rev feed and cryogenic cooling).

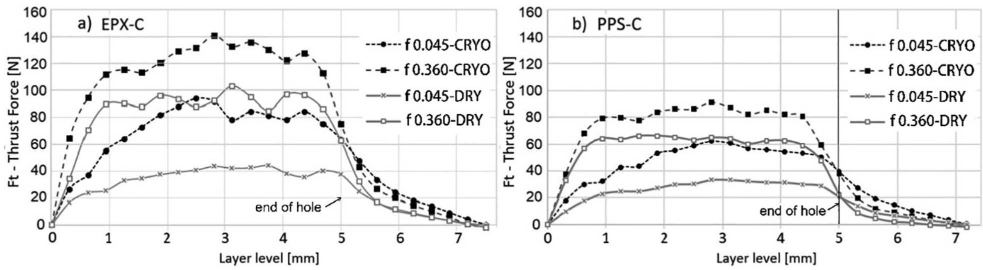

Fig. 5. Thrust forces under dry and cryogenic cooling for (a) EPX-C and (b) PPS-C materials.

i.e. higher for EPX-C material. Comparing the cooling methods, LN_2 imposes a torque 56% and 24% on average higher for EPX-C and PPS-C laminates, respectively. The torque values are lower for the PPS-C material, confirming the matrix is more ductile than EPX-C one. In dry method, the torque presents a constant and slight growth with drill feed, from 7.2 Ncm to 15.6 Ncm for EPX-C and 12.4 Ncm to 21.8 Ncm for PPS-C. In the cryogenic method the torque presents some variation when increasing the tool feed; after 0.180 mm/rev feed the torque decreases slightly. These results agree with the reduction of the cutting energy, as well as with F_d and UCF values, manly for EPX-C, as will be shown ahead.

Specific feed energy (U_f) and the specific cutting energy (U_c) are plotted, respectively, in Figs. 7 and 8, calculated according to the Kienzle model [31]. Kienzle's constants (k_{s1} and z) were obtained for PPS-C and EPX-C materials and for dry and cryogenic conditions. This model allows to calculate the specific pressure and cutting force for any cutting thickness. In the case of drilling, Kienzle´s constants were determined by linear regression of the measured torque (Mt) and thrust force (Ft), respectively, for specific cutting energy (U_c) and specific feed energy (U_f). The cutting section was calculated by sum of the product between cutting thickness (h) and cutting width (b) for the first and second tool tip angles.

Cutting thickness is a function of feed per revolution. In Figs. 7 and 8 is remarkable that U_f and U_c increase exponentially for feeds lesser than 0.090 mm/rev. The grey regions in these graphs represent feed ranges where the cutting thickness (h) is lesser than the cutting edge radius r_e = 39.5 μm (average between 60° and 130° lips angles). In these regions, an extremely compressive stress takes place in the workpiece material due to the small shear angle (φ), and the chip formation becomes more difficult. Besides low cutting thickness to edge radius ratio (h/r_e), shear angle (φ), and clearance angle (γ) contribute to push down the workpiece material. The stiffness increased by cryogenic method amplifies this phenomenon, and the EPX-C material is more susceptible to this effect (Fig. 7).

Specific feed energy (Fig. 7) is greater than specific cutting energy (Fig. 8) given that plowing (strain) prevails over cutting (shearing). In

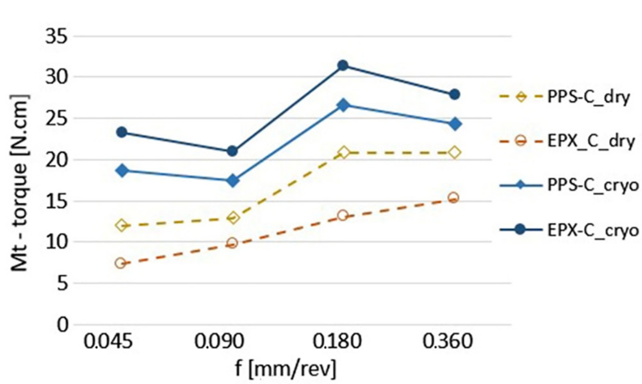

Fig. 6. Maximum torque as a function of the drill feed.

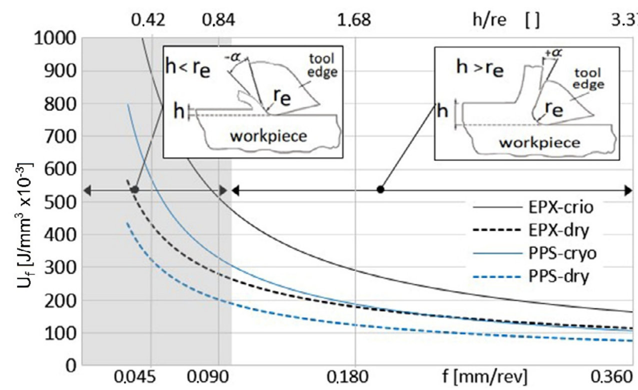

Fig. 7. Specific feed energy *vs* drill feed and cutting thickness/drill edge radius (h/r_e).

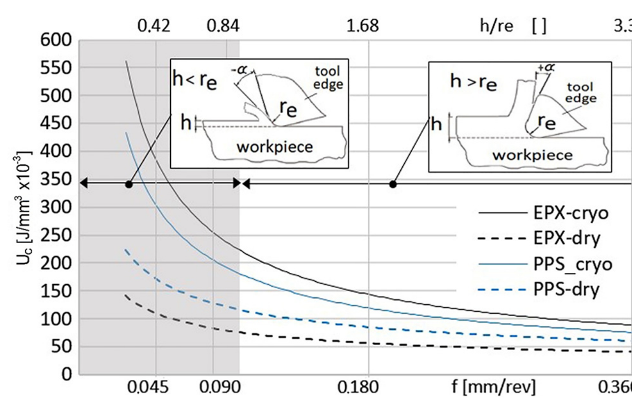

Fig. 8. Specific cutting energy *vs* drill feed and cutting thickness/drill edge radius (h/r_e).

other words, compressive stress caused by the chisel edge and negative rake angle near the tool centre is prevalent over shearing stress generated by cutting (lips and positive rake angle). In addition, the cutting speed is not enough to promote the cutting near the centre of the drill (chisel edge). Finally, drill feed reduction is not helpful to decrease the compression due to the size effect caused by h/r_e ratio.

3.2. Delamination

Table 4 presents the Analysis of Variance (ANOVA) for F_d results. The cooling method showed significance at the entry and exit of the holes, i.e., LN_2 worked the entire drilling operation. The feed (f) presents significance only at the hole entrance, instead the composite material presents significance at the hole exit. ANOVA shows significance for the interaction between cooling method and workpiece material, confirming the influence of the LN_2 over the composite.

Table 4
ANOVA for delamination at the entrance and exit faces of the hole.

	Entrance							Exit						
	SS	DF	MS	F	p	PCR	SGF	SS	DF	MS	F	p	PCR	SGF
Intercept	78.89	1	78.89	6127.4	0.00000		–	74.94	1	74.94	6363.8	0.00000		–
f	0.284	3	0.095	7.35	**0.00060**	23%	medium	0.018	3	0.006	0.52	0.66933	2%	insignif.
cooling	0.361	1	0.361	28.01	**0.00001**	29%	medim	0.220	1	0.220	18.66	**0.00012**	19%	medium
material	0.015	1	0.015	1.20	0.28006	1%	insignif.	0.155	1	0.155	13.19	**0.00089**	13%	medium
f*cooling	0.012	3	0.004	0.30	0.82655	1%	insignif.	0.026	3	0.009	0.73	0.54323	2%	insignif.
f*material	0.031	3	0.010	0.80	0.50023	3%	insignif.	0.012	3	0.004	0.35	0.78999	1%	insignif.
cooling*material	0.076	1	0.076	5.92	**0.02023**	6%	low	0.321	1	0.321	27.27	**0.00001**	28%	medium
Error	0.451	35	0.013			37%	–	0.412	35	0.012			35%	–

SS: Sequential Sum of Squares. DF: Degrees of Freedom. MS: Adjusted Mean Square. F: F-Test and P: Value of Probability.
PCR: Percent of Contributions Ratios and SGF: Significance.

Thermoplastic material (PPS-C) was susceptible to cryogenic action in which differences for delamination factor were verified between hole entry and exit (Figs. 9b and 10b).

Fig. 9a and Fig. 9b exhibit the effects of feed and cooling method, respectively, over the entrance F_d. In Fig. 9a F_d increases due to the growth of feed for both cryogenic and dry conditions given an increase of thrust force as previously showed in Fig. 5. As the feed rises the tool tip and the chisel edges impose more impact to the first composite layers, detailed in Fig. 4 (step I), working as an indentation, then a crack initiate. According to Won & Dharan [32], a half of thrust force is concentrated on the chisel edge. Furthermore, the subsequent layers work as support such as verified by Qiu et al. [33]. This is accentuated in the cryogenic cooling that increases the workpiece material stiffness, as previously mentioned, and the entrance delamination grows. LN_2 improves the overall stiffness and the PPS-C material is more susceptible to a damper reduction. As it will be seen in Section 3.5, Fig. 15c and Fig. 15f show cracks in fibres and delamination, respectively, for dry and cryogenic methods when drilling PPS-C material. It is remarkable the debonding of fibres bundle and delamination for cryogenic method.

Even enhancing delamination, the increase in drill feed did not affect statistically the F_d at the exit side (Fig. 10a and Fig. 10b), contradicting Hocheng & Tsao [19] in which growing in F_d was significant. In this current paper this non-significance occurred because the thrust forces at the hole exit (5 mm workpiece thickness) were quite similar (Fig. 5a and Fig. 5b). Instead, F_d in the cryogenic method is slight greater than in the dry method. Differently from hole entrance, the exit side does not have support due to the few and last plies. Thus, despite the compressive stress of the chisel edge, the indentation does not take place given the lack of support. As aforementioned, the thrust force grows as the feed rises, instead, the specific feed and cutting energies reduce as the feed increases. On average F_d at exit side is quite constant when increasing drill feed. In the same trend of entrance, the cryogenic method increases F_d and the PPS-C material is more susceptible to the LN_2 application (Fig. 10b).

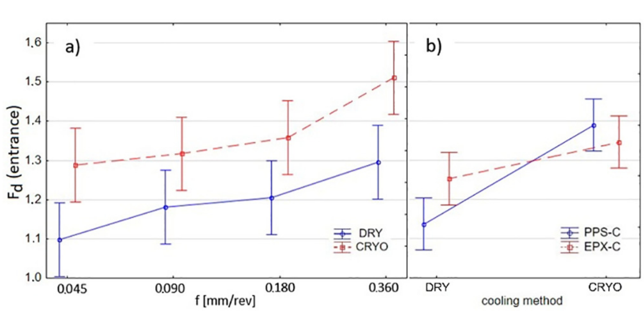

Fig. 9. F_d at the hole entrance: interaction effects for (a) cooling method *vs* drill feed and (b) material *vs* cooling method.

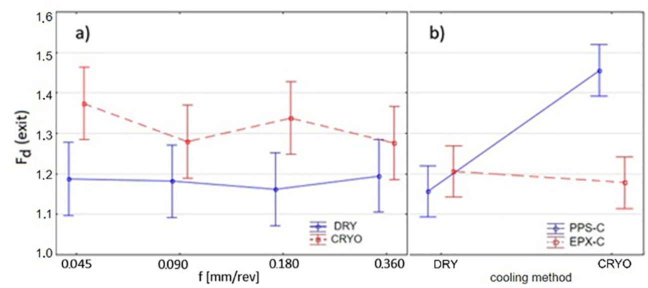

Fig. 10. F_d at the hole exit: interaction effects for (a) cooling method *vs* drill feed and (b) material *vs* cooling method.

3.3. Uncut fibres

Table 5 presents the Analysis of Variance (ANOVA) for UCF results. Different behaviours occurred at the entrance and exit of holes, despite the feed is predominant for both entrance and exit of holes. Significant 2nd order interactions were identified only at the hole entrance.

At the hole entrance (Fig. 11a and Fig. 11b), the application of the LN_2 keeps UCF near zero for the both workpiece materials. For the EPX-C laminate the UCF rises after 0.090 mm/rev feed. This means that the cryogenic cooling was helpful to retard the UCF initiation or tool feed higher than 0.090 mm/rev is fast enough so that LN_2 does not act over the cutting in EPX-C.

Differently from the delamination, to which the PPS-C composite is more susceptible, the UCF values remain steady with cooling method with UCF near zero at the entrance for this material (Fig. 11a). On the other hand, in the EPX-C composite LN_2 slight reduces the UCF at the entrance side. The increase of stiffness due to the LN_2 leads to a fragile fracture of fibres causing more delamination than uncut fibres in the EPX-C laminate. By contrast, in the dry condition the fibre bends inside the matrix and some of them remain uncut after drilling, as it will be shown in Section 3.5 (Fig. 17b).

Comparing UCF results at the hole entrance and exit, respectively, Figs. 11 and 12, it is noticeable that the UCF values are lower at the entrance side. Regardless of tool feed, UCF is lower because the tool secondary edge is always in contact with the hole entrance border throughout drilling process, thus the remaining fibres at the entrance will be cut by the drill secondary edge.

At the exit side (Fig. 12a), UCF indexes reduce as the drill feed increases after 0.090 mm/rev feed for PPS-C and after 0.180 mm/rev feed for EPX-C composite. The increase in feed induces a bending stress to the last plies. Fig. 12b presents the quick-stop drilling images, in which the drill stops before the total retreat of its tip. Is noticeable that the fibre bundles were not cut but they were broken at the centre due to the compression stress caused by the chisel edge. The fibre bundles bent and broke at the centre of the hole. The drill pushes out the

Table 5
ANOVA for UCF at the entrance and exit faces of the hole.

	Entrance							Exit						
	SS	DF	MS	F	p	PCR	SGF	SS	DF	MS	F	p	PCR	SGF
Intercept	0.154	1	0.15	83.2	0.00000		–	4.945	1	4.94	290.2	0.00000		–
f	0.029	3	0.010	5.27	**0.00417**	8%	low	0.743	3	0.248	14.54	**0.00000**	49%	high
cooling	0.062	1	0.062	33.36	**0.00000**	17%	medium	0.024	1	0.024	1.40	0.24460	2%	insignif.
material	0.106	1	0.106	56.88	**0.00000**	29%	medium	0.012	1	0.012	0.69	0.41177	1%	insignif.
f*cooling	0.011	3	0.004	2.01	0.12980	3%	insignif.	0.015	3	0.005	0.29	0.83276	1%	insignif.
f*material	0.047	3	0.016	8.43	**0.00024**	13%	low	0.106	3	0.035	2.06	0.12267	7%	low
cooling*material	0.048	1	0.048	25.64	**0.00001**	13%	low	0.028	1	0.028	1.65	0.20772	2%	insignif.
Error	0.065	35	0.002			18%	–	0.596	35	0.017			39%	–

SS: Sequential Sum of Squares. DF: Degrees of Freedom. MS: Adjusted Mean Square. F: F-Test. P: Value of Probability. PCR: Percent of Contributions Ratios and SGF: Significance.

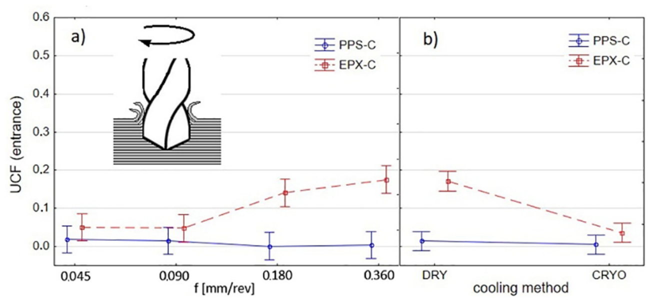

Fig. 11. UCF at the hole entrance: interaction effects for (a) material *vs* drill feed and (b) material *vs* cooling method.

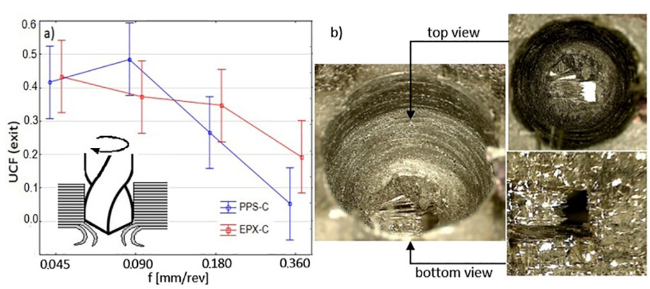

Fig. 12. UCF at the hole exit: (a) interaction effects between drill feed and material, and (b) details of the UCF initiation mechanism.

fibre bunches and at higher feed there is not enough time to the secondary edge cut these fibres, as happens in the entrance side. Thus, much more fibre connected to the composite material remains.

3.4. Hole diameter and roundness

Table 6 presents the ANOVA for the hole diameters and Fig. 13 exhibits the effects of the cryogenic and dry methods over such measurements at the entrance and exit of the holes (Fig. 13a and Fig. 13b). Xia et al. [16] identified dimensional variation in the diameter under dry condition and suggest that it is due to the thermal expansion, but they did not specify the polymeric matrix used. This hypothesis seems to proceed, however the thermoplastic PPS–C laminate presents a remarkable expansion of the diameter in dry condition, reaching 6.123 mm of the maximum exit diameter. On the other hand, the thermoset EPX-C did not show significant susceptibility to the cooling method. According to Fig. 13b, the dimensional results of the cryogenic drilling in the EPX-C material produced hole exit diameters smaller than nominal value, i.e., 0.4% interference when compared to a 6 mm standard pin. According to Zou et al. [28], this dimensional interference is already enough to impose a high frictional force during a pin fitting causing layer separation, and consequently pull out delamination. The cryogenic cooling yields an undesirable slight contraction for the thermoset epoxy/carbon material given the laminate relaxation [29], so that hole diameter shrinks with the drilling depth. Giasin et al. [14] verified the same relaxation effect in the glass fibre reinforced polymers (GFRP).

In dry drilling, when the temperature rises and overcomes the glass transition temperature (T_G), of the thermoplastic PPS matrix, the polymer become more ductile and its static friction coefficient increases as well [23]. Then the material is smeared over the hole wall surface and this causes perceptible unevenness at the surface, as shown in Fig. 15c. In addition to the identified thermal expansion, this unevenness contributes to the hole shape and consequent diameter variation. The thermoset composite (EPX-C) did not show significant susceptibility regarding the cooling method.

Table 7 presents the ANOVA for the hole roundness. Neither main factor nor interaction present significance at the hole entrance. Instead, at the hole exit the composite material and its interaction with cooling technique and drill feed were significant.

Fig. 14 shows the effect of the drill feed and cooling method on the roundness at the hole exit border. PPS-C composite is highly susceptible to the increase in temperature, thus at low feed (0.045 mm/rev) the higher friction time leads to a high roundness at dry drilling. The thermal expansion contributes to higher variability of hole diameter and consequently to a circular deviation. Shorter lengths of uncut fibres also contribute to worsen the roundness results, since they could not be dissociated during the measurement.

3.5. Scanning electron microscopy (SEM) analysis

SEM images were collect at the entrance and exit borders of the holes as well as at vicinity in order to help understand the damages in these locations. SEM images in Fig. 15 show the hole entrance border and their subsurfaces under dry method after drilling PPS-C material. The upper areas in the images correspond to the entrance face of drill. Fig. 15a does not present matrix absence and the surface right below the border is noticiable smooth. On the other hand, Fig. 15b presents some small regions of matrix absence. Furthermore, Fig. 15c shows in detail the fibre fracture at the hole border for 0.360 mm/rev feed. Thus, the high drill feed generated greater thrust force. When the chisel edge touches the workpiece material at the hole entrance, all the subsequent layers work as the support for the imposed compression [33], then the cracks are initiated, as presented in Fig. 15c.

Fig. 15d to Fig. 15f show the hole entrance border under cryogenic method. For 0.090 mm/rev drill feed the surface right below the border is smooth without damages. With 0.360 mm/rev feed, hole border clearly presents delamination (Fig. 15e and Fig. 15f), in which F_d value reached 1.52 (Fig. 9a). Given the enhanced stiffness of the workpiece

Table 6
ANOVA for diameter at the entrance and exit edges of the hole.

	Entrance							Exit						
	SS	DF	MS	F	p	PCR	SGF	SS	DF	MS	F	p	PCR	SGF
Intercept	1157.1	1	1157.1	823,125	0.00000		–	1168.5	1	1168.49	586,743	0.00000		
f	0.003	3	0.001	0.7	0.58962	5%	low	0.038	3	0.013	6.4	**0.00347**	19%	medium
cooling	0.002	1	0.002	1.4	0.25860	3%	insignif.	0.010	1	0.010	5.1	**0.03620**	5%	low
material	0.013	1	0.013	9.2	**0.00686**	23%	medium	0.075	1	0.075	37.7	**0.00001**	37%	medium
f*cooling	0.002	3	0.001	0.4	0.77203	3%	insignif.	0.002	3	0.001	0.3	0.81334	1%	insignif.
f*material	0.002	3	0.001	0.5	0.65467	4%	insignif.	0.039	3	0.013	6.6	**0.00304**	19%	medium
cooling*material	0.007	1	0.007	5.2	**0.03386**	13%	low	0.000	1	0.000	0.1	0.76367	0%	insignif.
Error	0.027	19	0.001			48%	–	0.038	19	0.002			19%	–

SS: Sequential Sum of Squares. DF: Degrees of Freedom. MS: Adjusted Mean Square. F: F-Test. P: Value of Probability. PCR: Percent of Contributions Ratios and SGF: Significance.

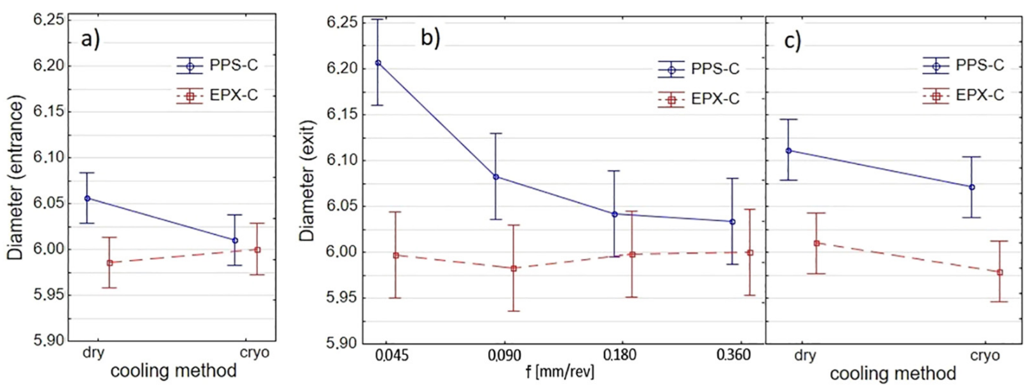

Fig. 13. Diameter (a) at the hole entrance and (b) at the hole exit.

Table 7
ANOVA for roundness at the entrance and exit edges of the hole.

	Entrance							Exit						
	SS	DF	MS	F	p	PCR	SGF	SS	DF	MS	F	p	PCR	SGF
Intercept	107,996	1	107,996	62.4	0.00000	–	–	398,501	1	398,501	69.324	0.00000	–	–
f	1474.1	3	491.4	0.28	0.83648	3%	insignif.	27,426	3	9142.0	1.5904	0.22474	9%	low
cooling	4163.3	1	4163.3	2.40	0.13751	9%	low	14,154	1	14154.0	2.462	0.13312	5%	insignif.
material	850.8	1	850.8	0.49	0.49184	2%	insignif.	29,222	1	29221.5	5.083	**0.03615**	10%	low
f*cooling	2683.6	3	894.5	0.52	0.67585	6%	low	6314	3	2104.6	0.3661	0.77824	2%	insignif.
f*material	4442.6	3	1480.9	0.86	0.48114	9%	low	82,899	3	27632.9	4.8071	**0.01176**	28%	medium
cooling*material	1339.0	1	1339.0	0.77	0.39019	3%	insignif.	30,320	1	30319.5	5.274	**0.03318**	10%	low
Error	32901.3	19	1731.6			69%	–	109,220	19	5748.4			36%	–

SS: Sequential Sum of Squares. DF: Degrees of Freedom. MS: Adjusted Mean Square. F: F-Test. P: Value of Probability. PCR: Percent of Contributions Ratios and SGF: Significance.

due to LN_2 cooling, the matrix did not damp the thrust force by causing fibres debonding and fracture. Furthermore, the surface right below the hole border present matrix absence and fibre pull out equally spaced.

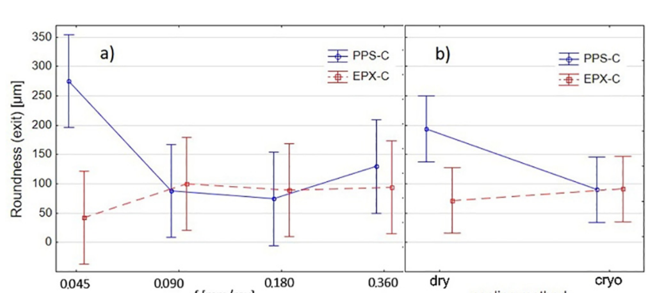

Fig. 14. Roundness at the hole exit: interaction effects for (a) drill feed and (b) cooling method.

Fig. 16 shows the hole exit in the PPS-C material. Fig. 16a and Fig. 16d present a smooth surface right below the hole border for both dry and cryogenic methods under 0.090 mm/rev feed. On the other hand, the surfaces right up the border (Fig. 16b and Fig. 16e) are matrix absence due to the higher drill feed (0.360 mm/rev). In the hole border drilled under dry condition at 0.090 mm/rev feed, the white areas correspond to matrix' burrs (Fig. 16a). With cryogenic cooling, the increase on matrix stiffness and consequent reduction on damper leads to a delamination instead (Fig. 16d and Fig. 16g). Furthermore, the higher cutting temperature under dry condition leads to matrix loss right up the yellow dashed line (Fig. 16c).

Fig. 17 exhibits the hole entrance border in the EPX-C composite. At 0.090 mm/rev drill feed (Fig. 17a and Fig. 17d) the surface right below the hole border presents smooth appearance when compared to dry and cryogenic drilling at 0.360 mm/rev feed. In dry condition

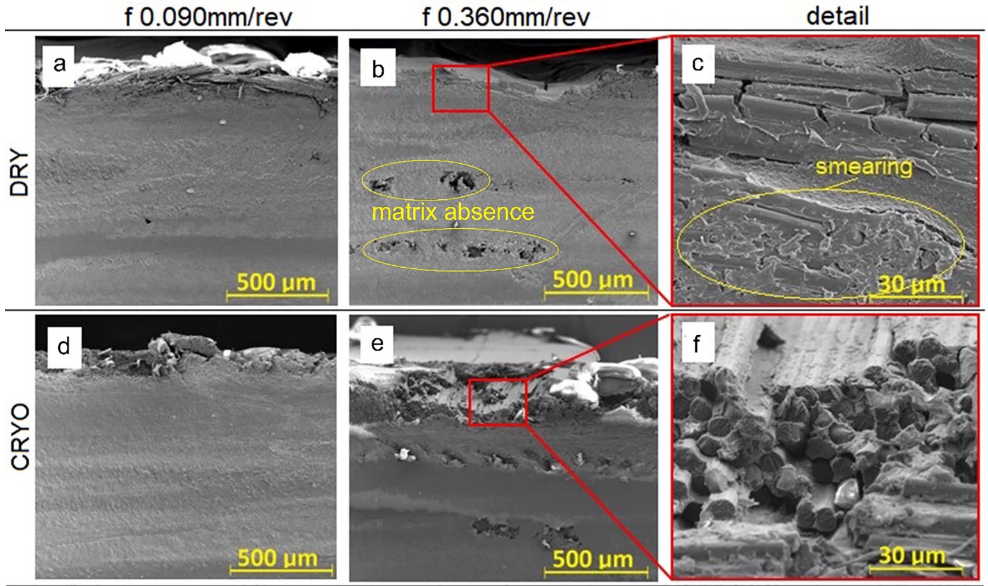

Fig. 15. SEM images at the hole entrance in PPS-C material.

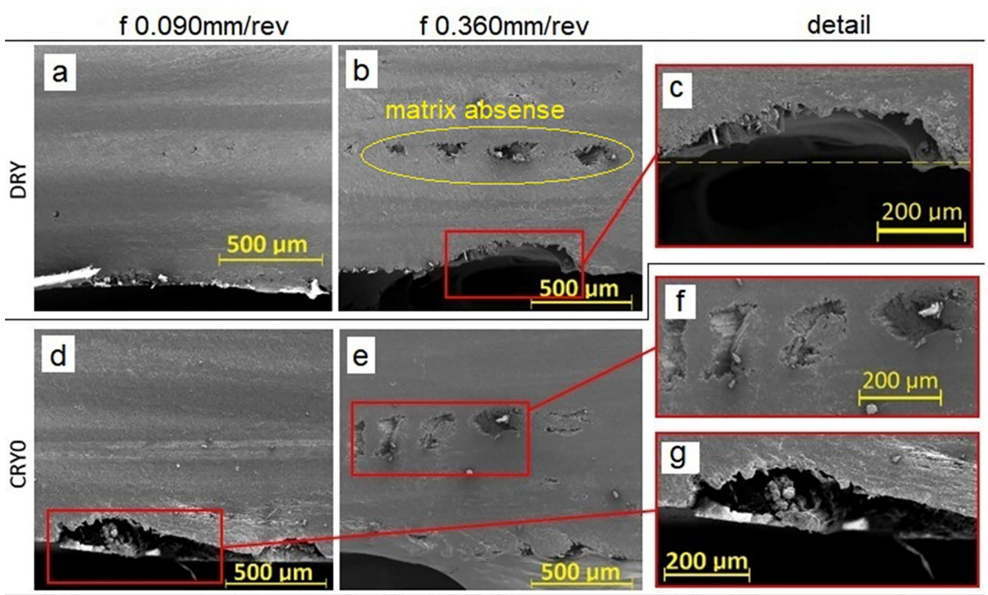

Fig. 16. SEM images at the hole exit in PPS-C material.

at the hole entrance (Fig. 17a to Fig. 17c) the matrix softening at hole entrance works as a damper which dissipates cutting energy and only few fibres detachments in the hole border took place. Furthermore, a few UCF at 0.090 mm/rev feed were observed (Fig. 17a), but they clearly occurred for 0.360 mm/rev (Fig. 17b). These findings corroborate the F_d and UCF results, presented in Figs. 9 and 11, respectively. On the contrary, LN_2 cooling (Fig. 17d to Fig. 17f) increases the matrix stiffness and consequently facilitates the crack initiation, which is detailed in dashed circles in Fig. 17d and Fig. 17e. For 0.090 mm/rev drill feed small delaminations were identified (dashed circle in Fig. 17d) while severe delamination at 0.360 mm/rev were prominent (dashed circles in Fig. 17e). Dry method softens the polymer matrix (Fig. 17c) and it appears like small fragments surrounding the fibres. Fig. 17f clearly shows the fibre-matrix debonding due to the differences in their thermal expansion coefficients (dashed circle), as also verified by Giasin et al. [14] under cryogenic drilling.

Fig. 18a to Fig. 18c portray hole exit borders of the EPX-C material drilled using dry method. For 0.090 mm/rev and f = 0.360 mm/rev drill feed slight push out delaminations a can be seen, thus confirming the F_d results in Fig. 10, that EPX-C composite is less susceptible to LN_2 than PPS-C material. Moreover, the surfaces right up the hole borders present matrix absence regardless of the drill feed. The higher cutting temperature due to the dry method produces a matrix smearing in the surface near the hole exit, as detailed in Fig. 18c above the dashed line. Matrix loss due to the of same heat effect can be clearly identified below the dashed line. Fig. 18d and Fig. 18f present the hole exit in the EPX-C laminate drilled under cryogenic cooling. Increasing matrix stiffness leads to a matrix loss in the wall right up the border (red

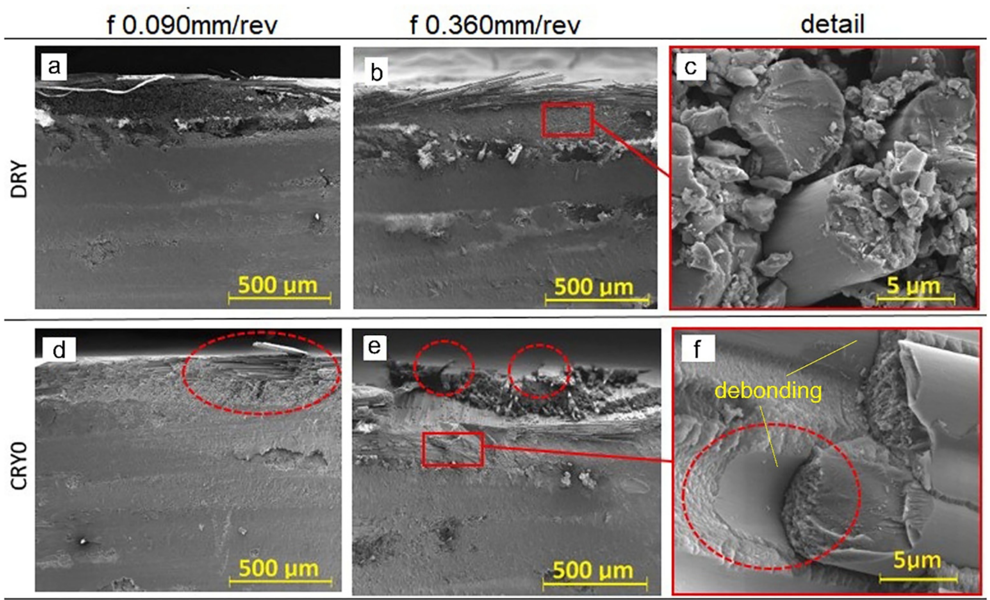

Fig. 17. SEM images at the hole entrance in EPX-C material.

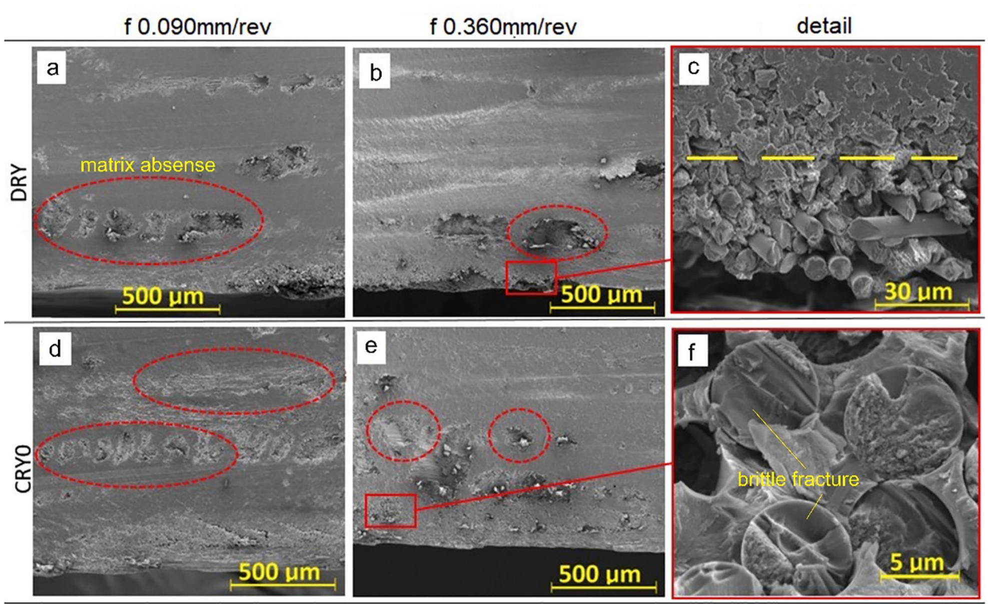

Fig. 18. SEM images at the hole exit in EPX-C material.

dashed circles). Fibres' cross sections present brittle fracture aspect under cryogenic cooling (Fig. 18f) while in dry conditions the fibres bend inside the matrix, as also reported by Zou et al. [34].

4. Conclusions

In this paper, cryogenic cooling was compared experimentally with dry drilling aiming to improve the quality of holes in thermoset and thermoplastic composites laminates. Thrust force, torque, specific feed and cutting energies, and scanning electron microscopy images were used to investigate and characterize damages, dimensional and geometrical variations of the holes. Statistical analyses determined the significant effects which were correlated to the outputs of drilling process. Thus, the main conclusions can be drawn as follow:

1. The cryogenic cooling increases stiffness of both composite laminate classes and, consequently, the drilling thrust force and torque. However, this effect partially improves the hole's quality.
2. The initiation mechanisms of delamination and uncut fibres aspects are different at the entrance and exit sides of the holes. At the entrance, the impact of drill tip against the rigid layers supported by sub adjacent ones produces more cracks and delamination. At the exit side, the lack of mechanical support for the last layers leads to uncut fibres.
3. The cooling method affect the drilling results in different ways for each composite material. The cryogenic strategy influence more significantly the thermoplastic matrix PPS-C laminate than the thermoset EPX-C material one with regard to the delamination factor (F_d).

4. Cryogenic cooling increases F_d at the hole entry and exit due the increase of both specific feed and cutting energy. This increase in F_d is higher for PPS-C than the EPX-C composite. Inversely, uncut fibres (UCF) are minimized manly at the hole entrance in the EPX-C material.
5. The cryogenic cooling maintains the drilled diameter close to the nominal value and minimize hole roundness in EPX-C composite.
6. PPS-C composite is very susceptible to the cutting temperature since it generates larger hole diameter expansion and higher roundness variation during dry drilling, mainly at the hole exit due to accumulated heat.

Credit authorship contribution statement

Marcelo Ferreira Batista: Conceptualization, Methodology, Writing - original draft. **Igor Basso:** Software, Validation, Investigation. **Francisco Toti:** Validation. **Alessandro Roger Rodrigues:** Project administration, Writing - review & editing. **José Ricardo Tarpani:** Resources, Formal analysis.

Declaration of Competing Interest

The authors declare that they have no known competing financial interests or personal relationships that could have appeared to influence the work reported in this paper.

Acknowledgements

The authors are grateful to Seco Tools and Semper Crio Industries for supporting this research.

Funding

This research received no specific grant from any funding agency in the public, commercial or not-for-profit sectors.

References

[1] Mathijsen D. Thermoplastic composites keep gaining momentum in the automotive industry. Reinf Plast 2016;60:408–12. https://doi.org/10.1016/j.repl.2015.06.095.
[2] Holmes M. Global carbon fi bre market remains on upward trend. Reinf Plast 2014;58:38–45. https://doi.org/10.1016/S0034-3617(14)70251-6.
[3] Fleischer J, Teti R, Lanza G, Mativenga P, Möhring H, Caggiano A. CIRP Annals - manufacturing technology composite materials parts manufacturing. CIRP Ann – Manuf Technol 2018;67:603–26. https://doi.org/10.1016/j.cirp.2018.05.005.
[4] Ben W, Hang G, Quan W, Maoqing W, Songpeng Z. Influence of cutting heat on quality of drilling of carbon/epoxy composites. Mater Manuf Process 2012;27:968–72. https://doi.org/10.1080/10426914.2011.610079.
[5] Davim JP, editor. Machinability of Fibre-Reinforced Plastics. 2015.
[6] Aurich JC, Kirsch B, Müller C, Heberger L. Quality of drilled and milled rivet holes in carbon fiber reinforced plastics 2014;24:56–61. doi:10.1016/j.procir.2014.08.008.
[7] Yashiro T, Ogawa T, Sasahara H. International Journal of Machine Tools & Manufacture Temperature measurement of cutting tool and machined surface layer in milling of CFRP 2013;70:63–9.
[8] Merino-Pérez JL, Royer R, Ayvar-Soberanis S, Merson E, Hodzic A. On the temperatures developed in CFRP drilling using uncoated wc-co tools part I: Workpiece constituents, cutting speed and heat dissipation. Compos Struct 2015;123:161–8. https://doi.org/10.1016/j.compstruct.2014.12.033.
[9] Khashaba UA. Drilling of polymer matrix composites: a review. J Compos Mater 2013;47:1817–32. https://doi.org/10.1177/0021998312451609.
[10] Schorník V, Zetková I. The Influence of the Cutting Conditions on the Machined Surface Quality When the CFRP is Machined 2015;100:1270–6. doi:10.1016/j.proeng.2015.01.493.
[11] Díaz-álvarez J, Olmedo A, Santiuste C, Miguélez MH. Theoretical estimation of thermal effects in drilling of woven carbon fiber composite. Materials (Basel) 2014;7:4442–54. https://doi.org/10.3390/ma7064442.
[12] Sorrentino L, Turchetta S, Bellini C. In process monitoring of cutting temperature during the drilling of FRP laminate. Compos Struct 2017;168:549–61. https://doi.org/10.1016/j.compstruct.2017.02.079.
[13] Barnes S, Bhudwannachai P, Dahnel AN. Drilling performance of carbon fiber reinforced epoxy composite when machined dry with conventional cutting fluid and with a cryogenically cooled tool. ASME 2013 Int. Mech. Eng. Congr. Expo., San Diego CA: 2013, p. 1–10.
[14] Jawahir IS, Attia H, Biermann D, Duflou J, Klocke F, Meyer D, et al. Manufacturing technology cryogenic manufacturing processes. CIRP Ann - Manuf Technol 2016;65:713–36. https://doi.org/10.1016/j.cirp.2016.06.007.
[15] Giasin K, Ayvar-soberanis S, Hodzic A. The effects of minimum quantity lubrication and cryogenic liquid nitrogen cooling on drilled hole quality in GLARE fi bre metal laminates. JMADE 2016;89:996–1006. https://doi.org/10.1016/j.matdes.2015.10.049.
[16] Biermann D, Hartmann H. Reduction of Burr Formation in Drilling Using Cryogenic Process Cooling 2012;3:85–90. doi:10.1016/j.procir.2012.07.016.
[17] Xia T, Kaynak Y, Arvin C, Jawahir IS. Cryogenic cooling-induced process performance and surface integrity in drilling CFRP composite material 2016:605–16. doi:10.1007/s00170-015-7284-y.
[18] Shyha IS, Aspinwall DK, Soo SL, Bradley S. International journal of machine tools & manufacture drill geometry and operating effects when cutting small diameter holes in CFRP. Int J Mach Tools Manuf 2009;49:1008–14. https://doi.org/10.1016/j.ijmachtools.2009.05.009.
[19] Hocheng H, Tsao CC. Effects of special drill bits on drilling-induced delamination of composite materials. Int J Mach Tools Manuf 2006;46:1403–16. https://doi.org/10.1016/j.ijmachtools.2005.10.004.
[20] Xu J, Li C, Mi S, An Q, Chen M. Study of drilling-induced defects for CFRP composites using new criteria. Compos Struct 2018;201:1076–87.
[21] Feito N, Díaz-álvarez J, Díaz-álvarez A, Cantero JL, Miguélez MH. Experimental Analysis of the Influence of Drill Point Angle and Wear on the Drilling of Woven CFRPs 2014:4258–71. doi:10.3390/ma7064258.
[22] Chen W-C. Some experimental investigations in the drilling of carbon fiber-reinforced plastic (Cfrp) composite laminates. Int J Mach Tools Manufact 1997;37:1097–108. https://doi.org/10.1016/S0890-6955(96)00095-8.
[23] König W, Graß P. Quality definition and assessment in drilling of fibre reinforced thermosets. CIRP Ann – Manuf Technol 1989;38:119–24. https://doi.org/10.1016/S0007-8506(07)62665-1.
[24] Saoudi J, Zitoune R, Mezlini S, Gururaja S, Seitier P. Critical thrust force predictions during drilling : Analytical modeling and X-ray tomography quantification Twist drill 2016;153:886–94.
[25] Caggiano A, Nele L. Comparison of drilled hole quality evaluation in CFRP / CFRP stacks using optical and ultrasonic non- destructive inspection Comparison of drilled hole quality evaluation in. Mach Sci Technol 2018;22:865–80. https://doi.org/10.1080/10910344.2018.1466330.
[26] Jia Z, Fu R, Niu B, Qian B, Bai Y, Wang F. Novel drill structure for damage reduction in drilling CFRP composites. Int J Mach Tools Manuf 2016;110:55–65. https://doi.org/10.1016/j.ijmachtools.2016.08.006.
[27] Kuo C, Wang C, Ko S. Wear behaviour of CVD diamond-coated tools in the drilling of woven CFRP composites. Wear 2018;398–399:1–12. doi:10.1016/j.wear.2017.11.015.
[28] Caggiano A, Nele L. Artificial neural networks for tool wear prediction based on sensor fusion monitoring of CFRP/CFRP stack drilling. Int J Autom Technol 2018;12:275–81. https://doi.org/10.20965/ijat.2018.p0275.
[29] Weinert K, Brinkel F, Kempmann C, Pantke K. The dependency of material properties and process conditions on the cutting temperatures when drilling polymers. Prod Eng 2007;1:381–7. https://doi.org/10.1007/s11740-007-0015-y.
[30] Mujahed Ahmad. Cryogenic Drilling of Kevlar Composite Laminated. 2004.
[31] O K. Die Bestimmung von Kräften und Leistungen an spanenden Werkzeugen und Werkzeugmaschinen 1952;94:299–305.
[32] Won MS, Dharan CKH. Chisel Edge and Pilot Hole Effects in Drilling Composite Laminates 2016;124. doi:10.1115/1.1448317.
[33] Qiu X, Li P, Li C, Niu Q, Chen A, Ouyang P, et al. Study on chisel edge drilling behavior and step drill structure on delamination in drilling CFRP. Compos Struct 2018;203:404–13. https://doi.org/10.1016/j.compstruct.2018.07.007.
[34] Zou P, Li Y, Zhang K, Liu P, Zhong H. Mode I delamination mechanism analysis on CFRP interference- fi t during the installation process 2017;116:268–77.